European Spine Journal (2022) 31:2831–2843
https://doi.org/10.1007/s00586-022-07353-1

ORIGINAL ARTICLE

Sacroiliac innervation

Hanno Steinke[1] · Toshiyuki Saito[2] · Janne Kuehner[1] · Uta Reibetanz[3] · Christoph-Eckhard Heyde[4] · Masahiro Itoh[2] · Anna Voelker[4]

Received: 7 March 2022 / Revised: 11 August 2022 / Accepted: 12 August 2022 / Published online: 27 August 2022

Abstract

Purpose To investigate the innervation pattern of the sacroiliac region, especially with regard to the sacroiliac joint (SIJ). Dorsal SIJ innervation was analyzed and described. Our main hypothesis was that nerves reach the SIJ dorsally, passing ligamental compartments, as this would explain dorsal SIJ pain.

Methods To examine sacroiliac innervation, we followed the nerves in over 50 specimens over several years. Plastinated slices were evaluated, nerves in the region were stained histologically, and the data were summarized as 3D models.

Results The Rami communicans and posterior branches of the spinal nerves and their branches that form a dorsal sacral plexus and communicating branches, together with corresponding vessels, were observed to form neurovascular bundles embedded by tiny fatty connectives in gaps and tunnels. Branches of L5-S1 pass the inner sacroiliac ligaments (the interosseous sacroiliac ligament and axial interosseous ligament). The outer sacroiliac ligaments (posterior sacroiliac ligaments, long posterior sacroiliac ligament, sacrotuberal ligament, thoracolumbar fascia) are passed by the S1-S4 branches. However, although the paths of these nerves are in the direction of the SIJ, they do not reach it. It is possible that impingement of the neurovascular bundles may result in pain. Moreover, the gaps and tunnels connect to the open dorsal SIJ.

Conclusion Our findings suggest that Bogduk's term "sacroiliac pain" correlates to "sacroiliac innervation", which consists of "inner-" and "outer sacroiliac ligament innervation", and to ventral "SIJ pain". The watery gaps and tunnels observed could play a significant role in innervation and thus in the origins of SIJ pain.

Level of evidence Individual cross-sectional studies with consistently applied reference standard and blinding.

Keywords Impingement · Entrapment · Sacroiliac joint · Sacroiliac pain · Ligament pain · Collagen

Introduction

The clinical entity "sacroiliac (**SI**) pain" may involve a yet unknown innervation pattern of the **SI** region, and especially of the dorsal **SI joint** (**SIJ**). To date, it is not known whether the **SIJ** is dorsally innervated, although it is accepted that the dorsal **SIJ** may be innervated due to clinical experience with anesthesia, because if nerves may not reach the **SIJ**, another explanation must be found for "**SI** pain".

✉ Hanno Steinke
steinke@medizin.uni-leipzig.de

Toshiyuki Saito
toshis@nms.ac.jp

Janne Kuehner
janne.kuehner@medizin.uni-leipzig.de

Uta Reibetanz
uta.reibetanz@medizin.uni-leipzig.de

Christoph-Eckhard Heyde
christoph-eckhard.heyde@medizin.uni-leipzig.de

Masahiro Itoh
itomasa@tokyo-med.ac.jp

Anna Voelker
anna.voelker@medizin.uni-leipzig.de

[1] Department of Anatomy, University Leipzig, Liebigstr. 13, 04103 Leipzig, Germany

[2] Department of Anatomy, Tokyo Medical University, 6-1-1 Shinjuku-ku, Tokyo 160-8402, Japan

[3] Department of Biophysics, University Leipzig, Härtelstr. 16-18, 04107 Leipzig, Germany

[4] Department of Orthopeadics, Trauma and Plastic Surgery, University Hospital Leipzig, Liebigstr. 20, 04103 Leipzig, Germany

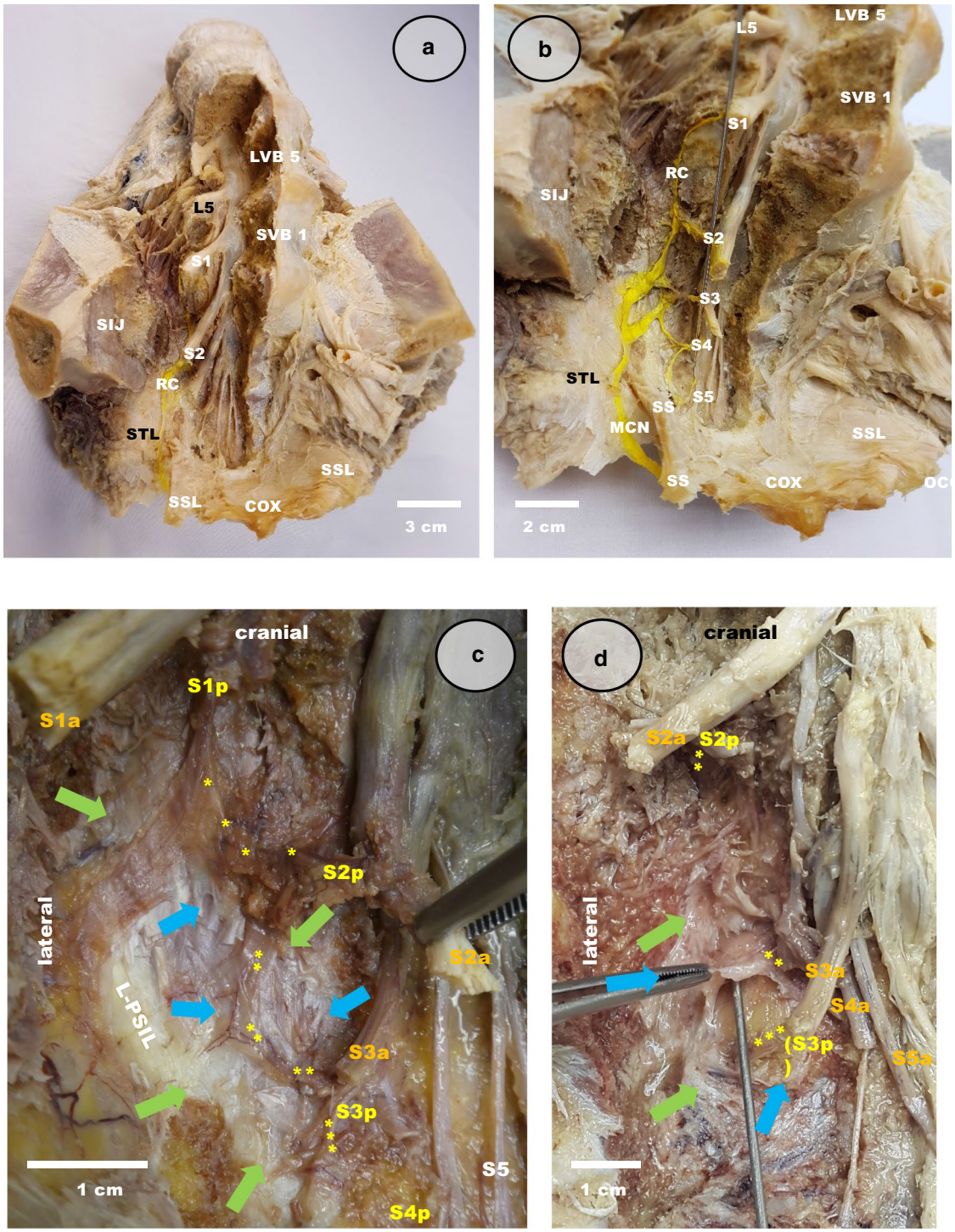

Innervation (and thus pain) should be related in general to spinal nerves, each of which divides into an anterior branch, a meningeal branch, and a **posterior branch of the spinal nerve** (**PBSN**) [1]. Some anterior branches are described to reach the ventral **SIJ** [1–7]; however, clinical and textbook opinion is that the **SIJ** is reached dorsally also, by **PBSNs** from L5 or L4 together with sacral **PBSNs** from the assumed S1-S3 segments [8].

PBSNs are thought to innervate muscles segmentally, not forming plexus. For the sacral muscles, this is textbook knowledge [8]. Several groups have described that lumbar **PBSNs** form plexuses [9–11]. Based on such contrary findings, there is still considerable debate regarding the innervation pattern of the sacral region [12]. Anatomical textbook knowledge often does not fit with the experiences of clinicians, leading them to ask which **PBSNs** may reach the

◂**Fig. 1** Dissection to the posterior branches of the spinal nerves (PBSNs). The dorsal sacrum in the ventral approach, anterior views, to observed the communicating branch (RC) between the lumbosacral PBSN. **a** Case L30 (♀ 80, formaldehyde-fixed). The spinal canal has been opened ventrally. On the right side, the bones have been removed to reveal the spinal nerves. On the left side, half of the 5th vertebra body (**LVB 5**) remains, as the sacral vertebrae, e.g., the 1st (**SVB 1**). The coccyx (**COX**) remains closed and attached to the sacrospinous ligament (**SSL**), which is partially removed on the right side for viewing the right sacrotuberous ligament **STL**. The right **SIJ** is opened. Lumbar and spinal nerves are revealed: **L5–S5** dividing into an anterior branch and a thinner **PBSN** (marked yellow). During dissection, an **RC** came into view (stained yellow). Some branches are directed toward the inner ligaments, dorsal of the **SIJ**. Thicker branches reach caudally, directed toward the outer ligaments, **STL**, and **SSL**. **b** Alternate view. This is a slightly more caudomedial view. A probe pushes the ventral rami ventomedially (**L5**, **S1**, **S2**, and **S3**) to enable visualization of the **PBSNs**. The **PBSN L5** is connected to the adherent segment **S1,** forming an **RC.** The **PBSNs S1**-**S5** are also connected (marked yellow). The **PBSN S4** and **S5** connection is very thin and merges to the ventral side of the **SSL**. All branches form plexus, giving rise to more branches. A medial cluneal nerve (**MCN**) is formed, passing medially, dorsally, ventral to the **SSL**, and to the medial dorsal side of the sacrum. **c** Case L31 (♀ 90, formaldehyde-fixed). Image obtained during the dissection process in ventral view. The anterior branches of the spinal nerves are labeled as **S1a**, **S2a**, and **S3a**. The segmental **PBSNs** are labeled accordingly: **S1p**, **S2p**, **S3p**, and **S4p**. **RCs** marked by stars (*). The **yellow** *** marks the **RC** between **S3p** and **S4p**. While the **S3a** is cut, the **S3p** can be seen connecting. The *** is covered ventrally by the sacral periosteum, marked by the **lower right green arrow**. This layer is seen still adhering to the not yet removed sacral bone (part of the medial sacral crest). The *** travels dorsally to it to reach the **S3p** (cannot yet be seen in this state of dissection). The **yellow** ** shows the **RC** between **S2p** and **S3p**. This ** is passing ventral to a vertical layer (**the lower blue arrow**), a flat aponeurotic structure for the erector (more cranial muscle fibers). A bony (periosteal) attachment is marked by **the lower left green arrow** (attaches to the lateral sacral crest, the remaining bone). To see the **, another aponeurotic layer must be cut (**upper blue arrow).** This layer arose from the removed bone with its periosteum and was ventral to **. The ** passes in a gap formed by the removed bone with periosteum and the aponeurotic layer (**upper blue arrow**). The fat of this region was removed to visualize the **;** however, the accompanying vessels remain. Branches of ** and accompanying vessels pass laterally toward ligaments which arise from the (removed) dorsal sacral periosteum: the **long posterior sacroiliac ligament** (**L-PSIL**) connecting shorter ligaments, which results in tunnels for the bundles to pass the **L-PSIL**. The bundles come to view laterally, left of the image. **Yellow** *: This **RC** connects segments **S1p** and **S2p**. However, a flat, fatty, not yet dissected block is seen immediately after removal of bone and periosteum. The aponeurotic erector (**upper blue arrow**) gives dorsal coverage to this fatty block, which bulges laterally (**X**), surrounding yet unseen branches of * (and vessels). Smaller branches from **S2p** and from * are directed toward **the AIL** and **ISL**. **d** An earlier stage of dissection than in Fig. 1c (same case: L31). **Yellow** **: This **RC** between **S2p** and **S3p** is ventrally covered by a periosteal layer (**upper green arrow**). A more dorsal erector layer is held by forceps (**upper blue arrow**). Note the fat, in which smaller vessels are embedded, accompanying the **. The erector layer covers the space dorsally to **. **Yellow** *** mark the path of the **RC** between **S3p** and **S4p**. A probe is positioned in the fatty space containing the *** with vessels. The origin of the erector held by forceps (**upper blue arrow**) now gives ventral coverage for the gap containing the ***. This erector layer connects caudally to the periosteum (**lower green arrow**). However, another erector layer is seen (**lower blue arrow**). This gives another dorsal coverage to the fat loose connectives containing ***. The ** and the *** therefore must curve laterally and convexly to reach the gaps formed by the erector aponeuroses and periosteum

dorsal **SIJ**, which dorsal **SI** ligaments they may pass, and why segmental pain is not seen in patients.

In a major study on sacral **PBSNs** conducted 20 years ago [13], Fortin et al. proposed an anatomical explanation for **SI** pain based on a dorsal **SIJ** innervation using clinical experiments, histological probes and fluoroscopically guided **SIJ** arthrography [14, 15], later followed by anatomical findings [16–18]. This aspect supports our hypothesis that nerves (and vessels) pass through gaps or tunnels inside dorsal ligaments, and that this may be of clinical importance for innervation, and thus for pain.

In this study, we investigated which branches of the **PBSNs** may play a role in this regard, which ligaments behind the **SIJ** they may reach or pass, and whether the **SIJ** itself is reached by any **RCs** or **PBSN** branches, all of which are aspects that have rarely been discussed in the literature.

A further question of this work is to think about the loose connective tissues and fluids in the gaps and tunnels behind the **SIJ** as described by Fortin, to find a possible explanation of why the application of anesthetics in these gaps is effective as a clinical treatment for "**SIJ** pain" [14, 15, 19].

Material and methods

51 human bodies were dissected either with a ventral or dorsal approach, at the University of Leipzig and the University of Tokyo. Online Resource 1 shows specific data of the body donors (e.g., age, weight). While alive, the donor had given consent for the use of body parts for scientific purposes at the respected Institute of Anatomy.

Dissection in the ventral approach

In total, 48 human specimens were dissected in ventral approach (Fig. 1; Online Resource 1). Forty-three fixed German human specimens (Institute of Anatomy, of Leipzig University; nine alcohol fixed [20, 21], 25 fixed using 1.85% aqueous formalin solution) and five formaldehyde-fixed Japanese human specimens (Department of anatomy, University Tokyo; all fixed using 1.85% aqueous formalin solution) were dissected to locate the **PBSNs** from the root to the periphery (Online Resource 1: number L1–L43 and T1–T5). 10 cases were dissected in the fresh post mortem situation, and one case after Thiel's fixation [22]. After opening the spinal canal, the fourth and fifth vertebral body and the sacral bone were removed until the branching **PBSNs** were found. Following these branches, the bone was consequently removed, and the posterior and **interosseous sacroiliac ligaments** (**ISLs**) were cut when necessary to follow the nerves, their connections, and further branching.

Dissection in dorsal approach

Having identified the location of the nerves, we dissected six specimens dorsally in order to validate our findings (Fig. 2; Online Resource 1). This included two unfixed, two Thiel-fixed [22], and two alcohol-fixed [20, 21] specimens. The **long posterior sacroiliac ligament** (**L-PSIL**) proved to be a key structure in quickly finding the **PBSNs** and their branches.

Plastination and histology

To ensure that the structures identified as communicating nerves per layout were actually nerves, we also evaluated them histologically. After treatment with alcohol and paraffin, the slices were stained for neurofilament (MAB 5262, Merck; 1:500) following standard procedures as HE and connective staining techniques (Online Resource 1). The slices were examined using a Zeiss AxioPhot 5 microscope (Zeiss, Oberkochen, Germany). Case L51 was an **SIJ** evaluation in a previous study [23] where PAS reaction was used [24]. For case 52, additional oblique slices were cut from a plastination block using metachromatic dye staining [25]. The serial sections of L51-L52 were evaluated macroscopically using polarized light microscopy (Zeiss AxioPhot) and scanned (Epson V750 pro, Epson, Seiko Epson Corp. 3-3-5 Owa, Suwa-shi, Nagano, Japan; Figs. 3 and 4).

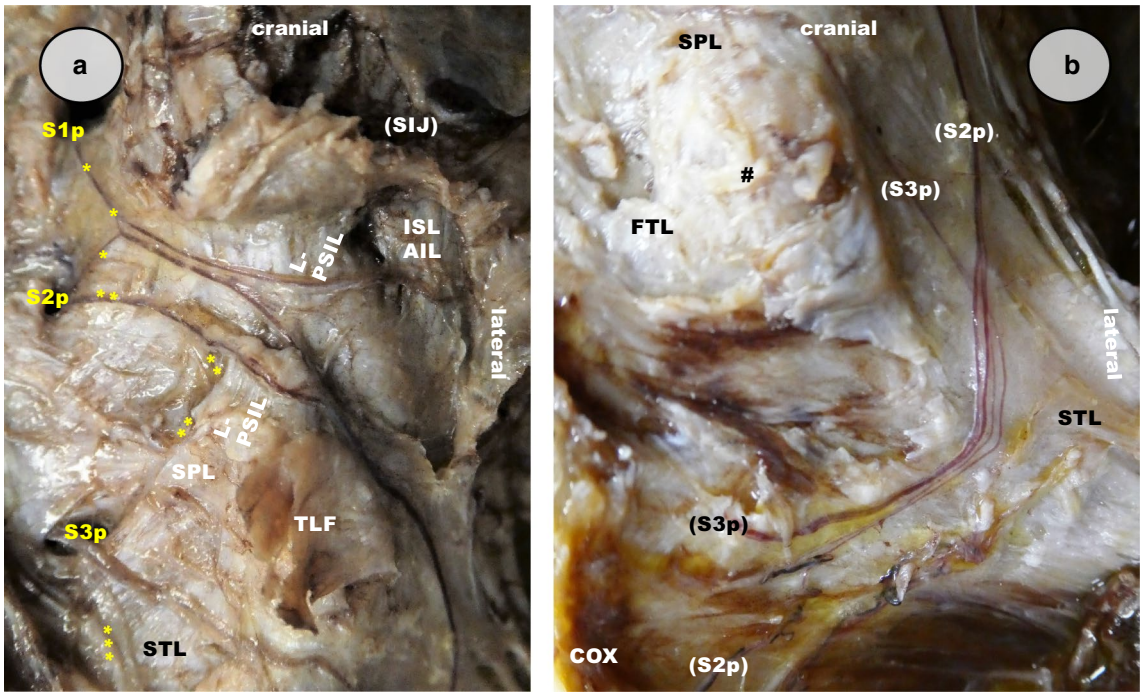

Fig. 2 Case 46 (♂, 90 years old, Thiel-fixed). Posterior branches of the spinal nerves **PBSNs** and their **Communicating branches RCs** in a dorsal approach. The erector origins are mainly cut off. The **long posterior sacroiliac ligament L-PSIL** is partly cut to see the nerves branching. The **thoracolumbar fascia TLF** was detached from the sacrum. Caudally, **a** sacral origin of the **sacrotuberous ligament STL** comes into view. It is also cut into parts. After removal of fat, the **PBSNs** are seen arising from the dorsal sacral foramina and are named according to their segments: **S1p**, **S2p**, **S3p**. a The **RC S1p-S2p** and its accompanying vessels are marked with yellow stars (*). Some fatty loose connectives remain. The ligaments are cut to visualize the *, vessels, and embedding fatty loose connectives. Dorsally the dissected **L-PSIL** is seen. Two branches of * with accompanying vessels pass dorsal to the periosteum and ventral to the cut short **PSIL**s. Neurovascular bundles pass here (L5-S1). A more dorsal layer touches the ventral side of the **TLF**, opened, flipped caudally. The upper branch of the * reaches laterally ventral to the **TLF**. One branch travels deeper, toward the **interosseous sacroiliac ligaments ISL** and **axial interosseous ligament AIL**, which however is still covering the hidden **SIJ**. The lower branch finds another connection to a direct branch of **S2p,** and a plexus is formed. The **S2p** and **S3p** form another **RC**, accompanied by vessels, marked with **. Again, parts of the **L-PSIL** and the **TLF** are partly cut to visualize parts of **. The **STL** remains intact, still dorsally covering parts of **. From **S3p,** another **RC** reaches caudally along with vessels, *** (to S4p; not seen). To see this branch, lamellas of the **STL** (or of the gluteal aponeurosis, which would be the same) are additionally removed. These are all perforated by tunnels for **RCs**, of which some are open and some are yet unseen. **b** At the region of the palpable **posterior inferior iliac spine PIIS (#)**, the **L-PSIL**, **STL**, and **TLF** merge. Nerves derived from communicating branches came into view after the gluteus maximus was removed from the **STL,** together with layers from which this muscle arises (the gluteal aponeurosis). These nerves are labeled as **(S2p)** and **(S3p)** according to the nearest segments. The **(S2p)** reaches more caudal than the **(S3p)**. **(S3p)** passes deep to **(S2p)**. Both branches reach caudally to the depth, then ventrally, and not to the dorsal surface, thus not forming the medial cluneal nerves. The target of both branches is the dorsal cranial **COX**, the ventral **SSL** (hidden), and the visible coccygeus muscle

Segmentation

For creating a 3D-model, CT images of cases L13, L24 and L51 were used for the segmentation of the pelvic ring and lower lumbar spine bones using the Materialise Mimics software (Materialise HQ, Technologielaan Belgium). Plastinated specimen were used for the spatial orientation (cases L50 and L52), as an MRI/CT/Plastinaton case (L51; Fig. 5; Online Resource 1). We introduced the data to Mimics as recently described [26, 27]. To create a virtual model of the dissected nerves, we chose five specimens representing the courses of nerves and their main variations (L18, L25, L29, L30, and L31) and measured the nerve branch lengths, the distances between branches as well as those between nerve connections and key structures. Using dissection images and the software's immediate 3D-preview in correlation to the plastinated specimen, we added the nerve structures to the CT slices.

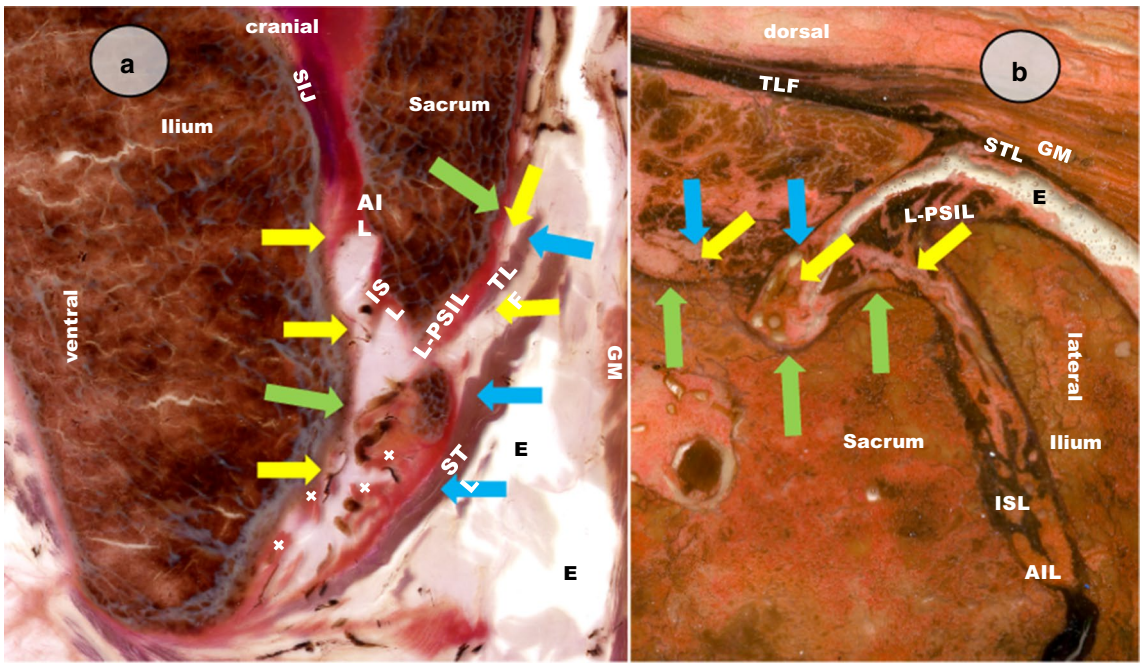

Fig. 3 Stained plastinated specimen cut through the region of the **SIJ, L-PSIL**, **PSIL** (**x**), the **TLF**, and the sacral origin of the **STL**. The **gluteus maximus** (**GM**) gives dorsal coverage. The **ISL** and **AIL** are marked dorsal of the **SIJ**. The periosteal layers are marked with **green arrows** and layers of the erector aponeuroses with **blue arrows**. Branches of the **PBSN** are passing between these layers and are marked with **yellow arrows**. **a** Case L51 (♀, 65). A serial section of a sagittal plastinated specimen near the **PIIS** stained by PAS reaction shows the distribution of sugars. This may indicate a collagen-type distribution [24]. The violet-stained cartilage of the **SIJ** can be seen cranially. No vessel or nerve is seen near the **SIJ**. The nearest vessel (with a nerve) is marked as **the upper left yellow arrow**. Dorsally the **AIL**, **ISL**, **PSIL,** and **L-PSIL** come into view**.** Blood filled vessels (brown) pass in the gaps between the sacrum and ilium, merged to the **ISL** with the **AIL**, ventrally and cranially to the **PSIL**, and to the **L-PSIL**. Accompanying nerves of these vessels can be anticipated due to their higher light refraction index and due to the bright color (**two left upper yellow arrows**) forming neurovascular bundles. Such bundles (**two right yellow arrows**) pass in gaps between the ventral periosteal layers, stained slightly orange (**the green arrows**). Layers of thinner and longer ligaments, such as the **L-PSIL**, are stained red. Some bundles pass between layers of the **L-PSIL** and **TLF** (**lower right yellow arrow**). Shorter ligaments near the periosteum form a common origin of the **L-PSIL, STL,** and **TLF**: **x**. The **L-PSIL** is interwoven with an aponeurotic origin for the **TLF** (the upper blue arrow), distinguishable after PAS reaction. Vessels pass with nerves in "empty" spaces, which contain loose connectives, of which the fat was dissolved by plastination. However, the spaces are not really empty, as loose connectives still remain. Empty (white) spaces can be seen marked with **E** in between the **TLF** and the **GM**, at the plastinated specimen dorsal border, below the artificially released **GM;** this really empty space occurred by incorrect embedding during the plastination process. **b** Case 52 (♀, 91). A horizontal slice cut from the block and stained with Giemsa [25]. Collagen stains overall as dark blue. The erector muscle remains red-brown, the aponeuroses are dark stained (**blue arrows**). Dorsally, the erector is covered by the **TLF**. Periosteal layers (**green arrows**) and the blue stained erector aponeuroses (**blue arrows**) form gaps in which vessels and nerves pass. From such neurovascular bundles (**left yellow arrow**), another bundle passes laterally to the **L-PSIL** (**left yellow arrow**). This nerve of the **RC L5/S1** and the accompanying vessels perforate the **L-PSIL**, pass the **ISL** (dark stained, dorsal to the gap between sacrum and ilium), and proceed toward the **AIL**. The joint (the gap at the lower right corner of the picture) is not reached by this bundle. The **GM** attaches to the **TLF** and to the **STL**. Due to plastination, an artificial white gap **E** occurred between the erector spinae, **L-PSIL** with ilium, and **STL** (the erector normally reach the L-PSIL). So, it is seen that the other gaps and tunnels are not empty—they are filled with loose connectives, which are not white, but stain pink. Neurovascular bundles pass in such spaces (yellow **arrows**)

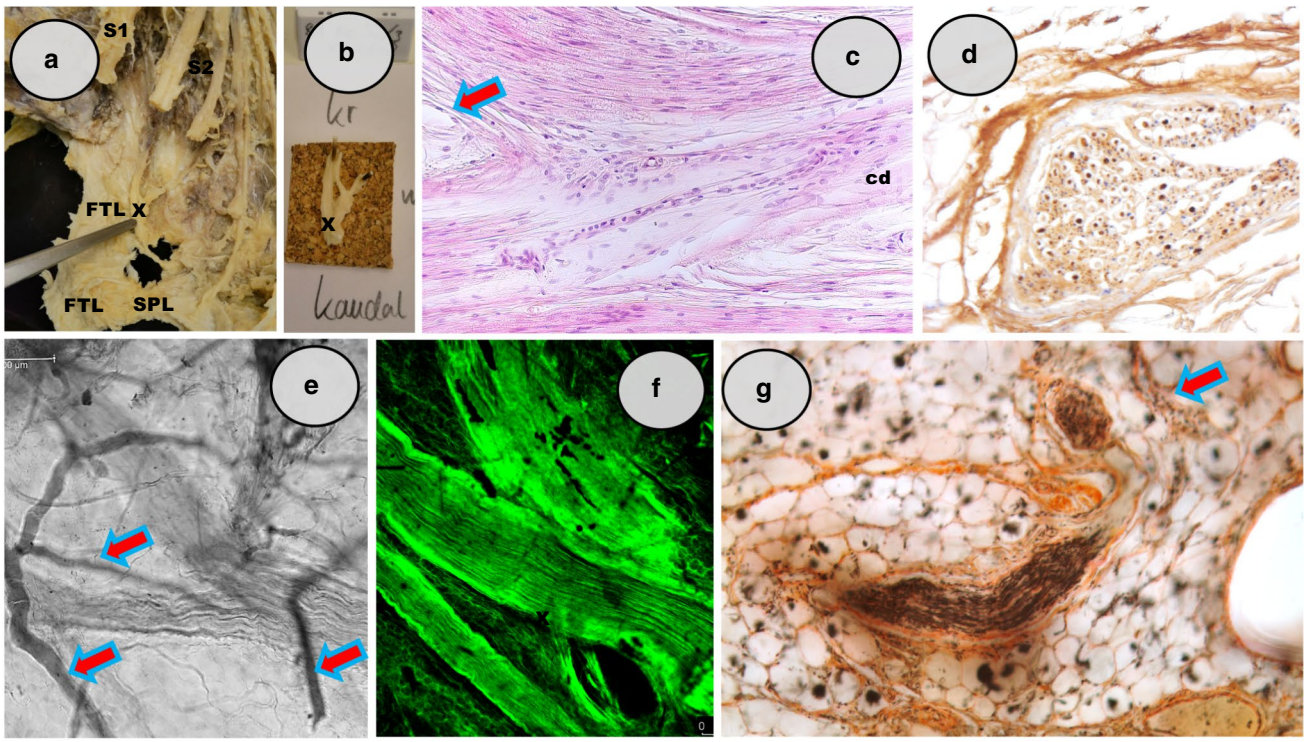

Fig. 4 Histology During dissection (Figs. 1 and 2), probes were taken to prove evidence of nerves reaching from the **PBSNs** and their **RCs** in the sacral region. **a** Removal for histology, case L18 (♂, 75). The cross of two **PBSNs** S2 and S3 is seen in the ventral view, held by forceps (**x**), removed from the more dorsal **TLF** and the **L-PSIL**. Branches of this cross perforate the ligaments. **b** Orientation, case L18 (♂, 75). The cross (**x**) was cut out and correctly assigned for histology. Kr = cranial, kaudal = caudal. **c** HE overview, case L29 (♂, 80). **HE** sections show thicker and thinner nerves merging one to another, dividing, and spreading again. A red-blue arrow indicates a vessel near the crossing nerves. cd = caudal. **d** Proof for nerves using neurofilament immunoreaction, case L29 (♂, 80).Positive precipitation (dark spots in the frontal cut nerve). The nerve is surrounded by looser fatty connectives. **e** Microscopic evaluation, case L31 (♀ 90). This specimen shows a doubled cross between L2 and L3. A bifurcation of an **RC** was removed during dorsal dissection (Fig. 1c, d). It is embedded to epoxy (E12) and investigated using polarized light. This makes it easy to find the higher refracting nerve branching. The nerves are seen by their curved form. Vessels are also nearby (red-blue arrows). The surrounding space is not empty, but structured, despite of the removed fat (due to plastination). **f** Auto-fluorescence, case L31 (♀ 90). The collagen layers of the RC emit auto-fluorescence after E12 plastination. The form of the nerves allows their differentiation from the surrounding connectives and fat, which are recognized by their lobular form. **g** Van Gieson staining, case L34 (♀ 57). The collagen layers surrounding the dark brown **RC** are stained orange. The nerve passes a thicker orange lamella in order to change direction. A small vessel accompanies nearby (red-blue arrow). The surrounding is fat.

Results

Based on the dissection, plastinated slices, histology, and the resulting models, we observed that the **PBSNs** and **RCs** spread in the direction of the **SIJ**, but do not reach it. Moreover, their paths perforate the **SI** ligaments.

Dissection in the ventral approach

All sacral spinal nerves could be followed in all cases except in cases L13 and T1 (2 of 48 cases; Fig. 1a, b; Online Resource 1). In this process, watery soft connective tissue and smaller accompanying vessels had to be removed. In all cases, **RCs** were revealed (Fig. 1b-d). The sacral **PBSNs** passes through the posterior sacral foramina and caudally reaches a fatty layer. Each PBSN was found to be connected by an **RC** to the lower segment **PBSN**, after another connective removal. The caudal **RC** of **PBSN** L5 to S1 pass from the L5 root at the intervertebral foramen L5/S1 to attach to **PBSN** S1 (Fig. 1a and b).

Thick aponeurotic lamellas arise cranially from the dorsal sacrum, where muscle fibers of the erector find these lamellas, seen ventrally after bone removal (Fig. 1c and d). Each periosteal layer gives root for a vertically aligned layer of the erector. On the cranial path, a **RC** has to encompass an aponeurotic layer laterally. The paths of the **RCs** result in a medial open concave arch (Fig. 5; Online Figure).

The gap for an **RC** is formed cranially open, caudally closed, open laterally for the downwards oriented part of the **SIJ**, and open medially for the emerging **SIJ**. Branches spread out laterally toward the **SIJ**; however, the joint itself was never observed to be reached by any nerve.

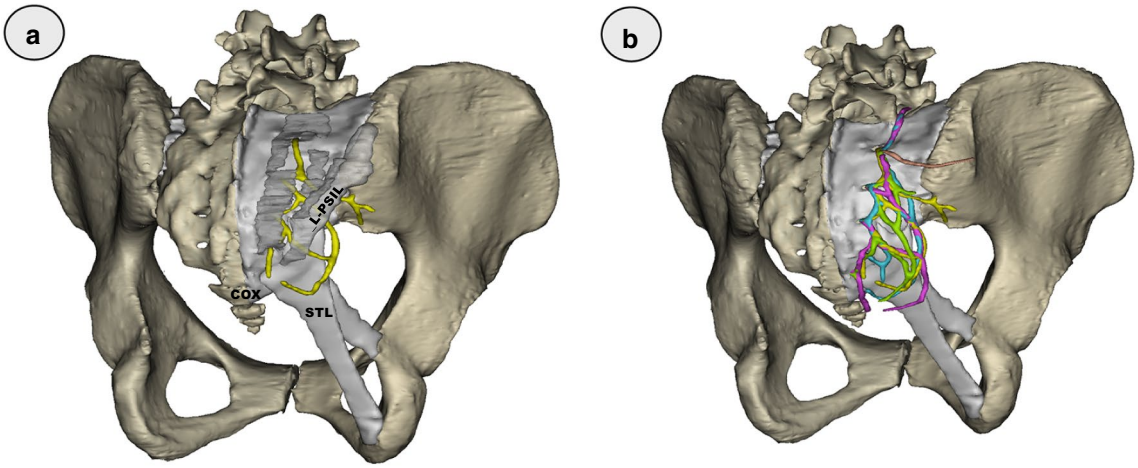

Fig. 5 **a** Reconstruction of **PBSNs** and their RCs in case L31 (♀, 90) to the bony and ligamental model of cases L 13, L24, and L51 in the dorsolateral view. The left ilium and sacrum are seen with the **ISL** (light grey). The right side of the sacrum is reconstructed with the covering masses of periosteum and short **PSIL**s (light grey). The **L-PSIL** is also marked in another shade of grey. The **TLF** attaches here. The aponeurotic erector origins are visualized as a darker semi-transparent grey. The communicating branches of case L31 are depicted as yellow arches, concave to medial, convex to lateral. Branches perforate and undercrosss the **L-PSIL**. The **STL** gives a pathway for further ramifications toward the region of the **COX**. **b** Summarized reconstruction of four cases (L18, L29, L30, and L31) to the bony and ligamental model of cases L 13, L24, and L51 in the dorsolateral view. This is the same reconstruction as in Fig. 5a but without the **L-PSIL** (Case L18 in green, L29 in pink, L30 in blue, and L31 in yellow). While position and number of communicating branches varies, the main layout is true for each **RC**. In a few cases a single branch belonging to segment S1 runs close to the **PSIS** (passing the **L-PSIL**) dorsal to the **SIJ**. This case is marked brown (case L25)

Dissections in the dorsal approach

After removing the covering of the thoracolumbar fascia (**TLF**) and muscle fibers of the erector, followed by the cutting of the longer and shorter dorsal **SI** ligaments, a **PBSN** and its **RC** become obvious, with further branches (Fig. 2).

These are seen perforating the layers of the short posterior sacroiliac ligaments and the long **ligament (L-PSIL;** Fig. 2a). To observe this, the **L-PSIL** has to be cut. The **RC** and plexus-like connections of the **RC** and the **PBSN** were observed in all cases. In the dorsal approach, the root of the medial cluneal nerves could be assumed as a result of plexus formation (Fig. 2b). Branches to the **sacrotuberous ligament** (**STL**) and the coccygeum were visible and passed through lamellas. Even after detachment of the gluteus maximus from the ligament, it was not clear if the branches of the **PBSN** reach this muscle's ventral surface. However, there are different layers or lamellas below the sub-gluteal gliding space, which may have layers covering the **STL**, and a lateral cranial fascial layer, which connects cranially to the gluteus medius. The nerves passing in these spaces with vessels reached from segment **PBSNs** S2 and S3 (Fig. 2b). They cross each other, S2 more superficially.

Distinguishing the **L-PSIL** from the **TLF** is not easy, because both rise together from the lateral sacral crest, deeper ligaments and the posterior inferior iliac spine (Fig. 2a). The **RC** branches, however, merge to this region, forming a plexus.

Plastination

Using plastination (3 cases; Fig. 3) compared to dissection data (49 cases Leipzig, 5 cases Tokyo = 54 cases; Figs. 1 and 2), the nerve branch pathways could be traced by looking for the always accompanying blood vessels. Nerves are visible as lesser brown structures and are distinguishable due to their higher refractive index (Fig. 3a). The vessels and the anticipated nerves pass in the gap between the ilium and the sacrum near the periosteum and in between the gaps of the periosteal layers and ligaments (Fig. 3a and b). Although the inner gaps seem to be empty at first, they are filled with looser connectives and fat (Fig. 3a, right bottom; Fig. 3b, artificial space between the **STL** and **L-PSIL**).

The **RC** of the sacral **PBSN** and their branching in between the sacral erector origins (Online Resource 1, Fig. 5).

RC L5/S1

In 27 of 57 cases (47%), in ventral approach 22 of 48 cases (52%), dorsal 2 of 6 (33%), seen in all plastinations. No doubled **RCs**.

Landmark PBSN L5: dorsocaudally, lateral to the superior articular processes of the sacral bone passing the iliolumbar ligament (not shown). Horizontal distance to the median line: 3–3.5 cm. **RC** to S1: directly caudolateral to the first posterior sacral foramen, 2.5–3 cm to the

median line toward the **SIJ** passing the **interosseous sacroiliac ligament** (**ISL**) and reaching the **axial interosseous ligament** (**AIL**).

RC S1/S2

52 of 57 cases (91%), ventral approach 45 of 48 (94%), dorsal approach 4 of 6 (67%; L44, L46, L47, L49), seen in all plastinates. A second (parallel) connection was seen in 13 of 54 dissections (24%; Fig. 2a).

Landmark PBSN S1: 2–5 mm caudal of the caudal parts of the **posterior superior iliac spine** (**PSIS**) at height of posterior sacral foramen II, ventral to the **L-PSIL**. Spread some millimeters caudally, 1 cm caudal to the most caudal part of the **PSIS**, ventral of the **L-PSIL**, approximately 1 cm caudal to the **posterior inferior iliac spine** (**PIIS**). Looping to the **STL**. The most lateral part is on a vertical line from **PIIS** to 1 cm lateral. Distance to the **PSIS**: 4–5 cm. Connection to **RC** S1 mostly caudal of the medial border of the **L-PSIL**, rarely laterally.

RC S2/S3

41 of 57 cases (72%), ventral approach 37 of 48 (77%), dorsal 4 of 6 (67%; L44, L45, L48, L49), seen in all plastinates. Parallel connection: 5 of 54 cases (9%).

Landmark PBSN S2: Divides early inside the 2nd posterior sacral foramen. **RC** S2/S3: 3rd posterior sacral foramen laterocranially, medial to the **L-PSIL**. Crossing **RC** S2 to **RC** S3: a field 2–3 cm caudal to the **PIIS**, i.e., 4–6 cm laterocaudal to the caudal parts of the **PSIS** (in two cases at **PIIS** height). Looping first medially, then dorsally toward the **STL**, level 5th sacral vertebra and coccygeum.

RC S3/S4

32 of 57 cases (56%), ventral approach 29 of 48 (60%) dorsal 3 of 6 (50%; L45, L46 and L48), in all plastinates. Three parallel aligned **RC** (6%).

Landmark PBSN S3: Divides inside the 3rd posterior sacral foramen ventrally to the **L-PSIL** and to the more superficial ligaments, crossing other nerves, dorsal near to the origin of the **STL** (Fig. 2b, Online Resource 2).

RC S4/S5

29 of 57 cases (51%), ventral approach 23 (48%) dorsal 3 (50%; L46, L48, and L49), in all plastinates. Small branches, thicker accompanying vessels. **RC** at a line 4th, 1 cm laterocaudally to the 3rd foramen.

Landmark PBSN S4: 3rd and 4th foramina vertically 2–2.5 cm to the median line. Branches superficially crossed by branches and plexuses from upper segments.

RC S5/Cocc

11 of 57 cases (19%), ventrally 9 (19%) dorsally one case (17%; L44), once seen in the plastinates (L56, Fig. 3a). Thin branch, thick vessels.

Landmark RBSN S5: 5th posterior sacral foramen al line 1.5 cm to median. Branches crossed by upper segments. Run caudally along the coccygeum.

Ramifications of the RC/PBSN

Further distal spreading seen in between the periosteal layers or ligaments, in gaps (Fig. 1b). There are ligamentous compartments (Fig. 1c, d) behind the **SIJ** that are in contact with the connectives in the wide gaps and thus indirectly with the nerve branches and accompanying vessels within. These are the **AIL** and **ISL,** reached by the **RC/PBSN** branches from L5-S1, in terms of an upward orientation of the branches perhaps coming from **S2** (Fig. 3, Online Resource 2).

Other branches (S1-S4/5) pass from the gaps to tunnels which perforate the **L-PSIL**, **posterior sacroiliac ligaments** (**PSILs**), **breves** et **longi**, the **TLF**, and final layers of the **STL** (Fig. 1c). From these, the nerves spread out distally and form other nerves, e.g., the medial cluneal nerves (Fig. 2b).

On their different paths, they also find others and form various types of plexuses (Figs. 1c, 4a and 5), with the final branches often crossing those from other segments (Fig. 2b).

Histology

To validate the dissection- and plastination-based findings, crossing branches of **RCs** were dissected and removed (Fig. 4a, b), and HE and immunostaining (Fig. 4c). We did not see cells at the **PBSN/RC** intersection. Immunostaining for neurofilament revealed the nerves (Fig. 4d). In slices, nerves are indirectly verified by their analog layout in dissections, and by their accompanying vessels, as seen submacroscopically (Fig. 3) or macroscopically (Figs. 1c, 2 and 3). Vessels accompany the **RCs** in spaces with looser connectives (Fig. 4e), connected by collagenous structures revealed by the auto-fluorescence of the outer looser connectives (Fig. 4f). The nerves were never free of vessels; neurovascular bundles were formed by such loose connectives in wider spaces (Fig. 4e, f, g). These bundles pass fatty connectives (Fig. 4c, e–g) that are structured, as the neurovascular bundles curve lateral to such connective lamella which are all embedded in fat (Fig. 4g).

3D segmentation

The findings were summarized in the form of a 3D model (Fig. 5).

Discussion

We follow Bogduk's clinical experience and his reasoning regarding the two entities that explain pain and innervation of the sacral region: "SIJ pain", and "ligament (lumbosacral) pain" [28]. Bogduk stated that "sacroiliac pain" encompasses both terms, an insight he gained from observations regarding anesthesia:" *Lateral branch blocks relieve pain from the posterior ligaments; they cannot block pain from the sacroiliac joint. Intra-articular blocks relieve joint pain; they do not relieve ligament pain*" [28].

We see the anatomical background for such clinical phenomenon in the form of gaps through which the nerves pass. More knowledge on what "SI innervation" means anatomically would allow clinicians to understand normal (painless) function. This was the intention of this study—to enable clinicians to address anatomical structures during their treatment.

To demonstrate the "innervation" of the sacro-iliac joint (**SIJ**) and the ligaments behind it, we first show nerves by dissections (Figs. 1, 2, 3, 4 and 5) and prove their existence (Fig. 4d).

However, for definitive proof of the term "**SIJ** innervation", it must be shown that nerve endings or synapses reach the joint, and this must also be true for a final proof of "**SI** ligament innervation". However, as in previous studies, this was not observed.

For the ventral parts of the **SIJ**, the term "innervation" is conducted by the research of Szadek's group [5, 6]. Their term "**SIJ** innervation" may be correct for the ventral side of the **SIJ**, despite even Szadek's experiments failed to demonstrate free nerve endings or synapses.

For the dorsal side of the **SIJ,** however, we refer here in regards to "innervation" to the viewpoint that the nerves and the structures they pass are not related to each other, since they are separated by connectives or fat (Figs. 1d and 2b), i.e., by the "empty" spaces observed histologically (Fig. 4f-d) or in plastinated specimen (Fig. 3). In this study, we found these spaces surrounding each branch, accompanied by vessels, thus forming neurovascular bundles. This is, thus, the anatomically "healthy" situation. The nerves pass in the gaps and tunnels, and may end there: The **SIJ** itself is not reached.

Approach

In dorsolateral approach, Fortin macroscopically observed branches of a communicating branch **RC** and of **PBSN S1** to **S4** [13]. These observations were already published [1, 29]. In our opinion, compared to the ventral approach (Fig. 1), the dorsolateral approach used by Fortin (Fig. 2) showed the nerve from the origin to the periphery, approaching dorsolaterally but not reaching the **SIJ**. By following the nerves, we can determine their relation to the ligaments in the 57 dissected cases using different approaches and in three serial plastination sectioning (Figs. 1, 2, 3, 4 and 5).

Existence of the sacral RC

We observed the **RC** in the sacral region as Fortin and others reported [1, 13, 29]. Despite high topographical variation (Fig. 5b), the general layout was consistent in all cases (Figs. 1, 2 and 3; Online Resource 2). In 30 cases, we could not see the **RC** L5/S1 (Online Resource 1). The sacral **RCs** are, however, continuations of the described lumbar **RC** [1, 9, 11, 12, 29]. The **RC L5/S1** was not in main focus here and may be an anatomical structure like the sacral and lumbar **RCs**. We also have hints for RCs connecting the **PBSN** in coccygeal region (11 of 57 cases, 19%).

Segmental (autochthonic) innervation is unlikely in the sacral region

The lumbar **PBSN** have recently been described to form a plexus [10, 11, 30]. In the sacral region, we also observed the **RC/PBSN** branches forming a plexus and connecting to the coccygeal branches (Figs. 1, 2, 4a, 5; Online Resource 2). Consequently, distinct segmental innervation of the dorsal sacral region also seems unlikely. The lumbo-sacral musculature of the erector, the ligaments seen here, and the skin can rarely be described as segmentally arranged (i.e., strictly "autochthonic" innervation).

Hungerfold's group reported delayed erector onset in patients with pain in the **SIJ** and muscles such as the gluteus maximus [31], and give a biomechanical explanation for this reactive onset.

We observed gaps of the erector (Figs. 1c, 3a) and layers of gluteal aponeurosis, as McGrath also have noticed [32], embedded in tunnels (Figs. 2b and 3b). Hungerfold's onset can be seen as a reactive change of the erector resulting in pressing or narrowing of the gaps seen here (Fig. 3b) resulting in a kind of entrapment. Interestingly, any widening of these gaps may be helpful, as yoga may help in **SI** pain [33].

Branches of RC/PBSN directing to the SIJ passing ligaments

A continuous gap without any capsule was observed dorsal to the joint cartilage and ventral to the **axial interosseous ligament** (**AIL**; Fig. 3). Fortin et al. described tunnel-like gap connections as follows: "*Dissections revealed nerve branches derived from the loops connecting **S1** to **S4** dorsal rami to the dorsal ligaments*" [13]. They did not observe branches to the joint, but to the ligaments; however, based on these data and the literature, the authors concluded that "*... the* **SIJ**…*is innervated* [dorsally, HS]" [13].

Our macroscopic findings cannot exclude dorsal innervation of the joint by branches of the **S2** or **S3**; our data on the path of the sacral **RC** branches also leave open the question of whether smaller **S2** and **S3** branches may reach the joint cartilage. The **RC S1/S2** and **RC S2/S3** were observed in 52 and 41 of the 57 cases, respectively, not ending to the **SIJ** (Online Resource 1).

Branches of RC/PBSN to "inner SI ligaments" ISL and AIL: segments L5-S1

Japanese literature describes a branch from the lumbar **PBSN L4** and **L5,** a branch reaching the **SIJ** region cranially, quoted, but not seen by Fortin [13]. We observed the **L5** branch connecting to **S1** in approximately half of the cases (47%, Fig. 1b, Online Resource 1; [12]). This branch passes the iliolumbar ligament [34], before possibly branching elsewhere near to the cranial **SIJ**. Dorsal of the joint, we see smaller nerves of **RC/PBSN** segments **L5** and **S1** passing the **interosseous sacroiliac ligament** (**ISL**) and targeting the **AIL** (Fig. 3). Based on our dissections, compared to the plastinated specimen (Figs. 1, 2, 3, 4 and 5), we underline Fortin's description of these **RC** branches reaching the **AIL**, a relatively weak and small part of the **ISL** near the joint [13, 35]. The nerve fibers in the gaps could explain **ISL/AIL** pain due to **L5** and **S1**, referred as sciatic pain, and not "innervation of the **SIJ**" as Vilensky and Fortin claim [16, 17]. Our findings provide however a hint for "*inner SI ligament innervation*" of the region near the joint cartilage, as of the **ISL** and **AIL**; arguments for "ligament innervation" with referred sciatic pain as an anatomical explanation for Bogduk's clinical term "ligament pain" [28].

Branches of RC/PBSN directing "outer SI ligaments" L-PSIL, the PSILs, TLF, and STL: segments S1-S4

Neurovascular bundles are seen passing through fat-filled flat tunnels inside the voluminous ligamentous complex behind the **SIJ** and medial to the **long posterior sacro iliac ligament (L-PSIL)**, grouped together to form the shorter ligaments, **PSIL** (Figs. 1c, 2, 3, 4a, 5; [27]).

McGrath's group reported that these nerves run from gaps to small holes that perforate the **PSIL** and branch to the **L-PSIL** [32]. We also observed **PBSN/RC S1**, **S2,** and **S3** branches that perforate the **L-PSIL** laterally (Figs. 1, 2, 3 and 5).

The **L-PSIL** as part of the **PSIL** [27] has been proposed as pain generator [7, 32]. As McGrath et al. described three layers [32], we see these main layers with their neurovascular bundles passing in small fatty gaps in between the **L-PSIL/PSIL** compartment, identifiable by their accompanying vessels (Figs. 1c, d, 2, and 3).

The neurovascular bundles cross and twist (Fig. 2b, Online Resource 2). We have reported that the **sacrotuberous ligament STL** twists for some functional reasons [26]. However, both the twisted nerves arise earlier from the plexus, which makes more precise segmental assignment very difficult, except for the general statement of their main origin from **S1-S4** and their targeting of such "*outer" SI ligaments*".

"SIJ innervation" and "SI ligament innervation" correlates to "SIJ pain" and "SI ligament pain"

Ventral branches of the **SIJ** are emphasized to reach and thus innerve the ventral **SIJ**, i.e., the ventral capsule, near the cartilage, along with branches of the anterior branch of the spinal nerve **S2** [1, 6, 17, 36]. Cranially, the joint may be reached by **PBSN L5** [1, 9, 10, 12, 13].

When nerves may not reach the dorsal **SIJ**, as we describe here, pain described by Bogduk as "ligament pain" could arise from ligaments or from the nearby connectives. These connectives are initially seen as to be "filling" the ligament gaps, due to the gliding and rotational movements involving the **ISL**, **L-PSIL**, and **PSIL** [28, 37, 38]. During these movements (of less than 0.5 mm and 1°, respectively), the **RC** passes in a nearly motionless region medial to the **L-PSIL** under normal conditions (Figs. 1c, d; 3).

The neurovascular bundles are located like an eye of cyclone inside these loaded ligaments. The arising medial cluneal nerves, for example, could become entrapped as they pass through the **ISL/AIL** compartments, as described by Konno et al., resulting in multiple type of pain (Fig. 1c) [39].

Also the **SIJ** itself is described to be a main pain generator [19, 40]. The data from the literature and our research suggest that not only the (ventral and cranial) joint itself, but also the dorsal compartments of the **SI** region seen here could be such generators, as McGrath, Vleeming, and others have suggested for the **L-PSIL** [7, 32]. We think that the *inner* and *outer ligaments* may be considered as dorsal parts

of the **SI** region, due to the open dorsal anatomy; there is no dorsal synovial ending of the joint.

Neurovascular bundles in the gaps and tunnels behind the SIJ

A correlation between the width of the gaps and adequate anesthesia has already been established [41]. Thus, the gap itself may provide information about the fat-embedded **PBSN/RC** branches (Fig. 4d). Comparable nerve entrapment syndromes are thought to occur for the medianus and ulnar nerves, as well as for nerves of the size seen here, perforating the abdominal wall [42, 43].

Ischemic endoneural vascularity damage may also apply to the nerves seen here, passing the "*inner*" and "*outer SI ligaments*".

The **RC/PBSN** branches with their vessels and loose connectives are surrounded by thicker masses of collagen (Figs. 3a, 4f; Online Resource 2) [23, 44, 45]. We know that collagen induces piezoelectrical potentials [46], and that collagen consists mainly water, not protein—a tendon consists of 62% water [47]. Highly structured water may explain this piezoelectric effect of collagen, which may have an impact on the **RC/PBSN** (Fig. 3). In the healthy anatomical state, no pain is induced because the bundles are freely embedded.

These structural masses of collagen surrounding the **RC/PBSN** bundles have another general but unexplained property. Ott's group, and others, have shown that a "dead", watery, cell-free collagenous matrix can be made functional by foreign blood [48, 49]. This "matrix" has a defined anatomy, which we see here poor in cell number (bradytrophic) surrounding and even building the **RC/PBSN** bundles with collagen, fat, and (synovial) water (Figs. 3a, 4). With Ott's experiments in the background of our thinking, the collagen, and water (which synovia and collagen mainly consists of) should be considered regarding "**SI** innervation" [48, 49].

If we are correct, the synovial milieu—the soft, fluid matter surrounding the **PBSN/RC** near the "*inner ligaments*"—plays a role in joint homeostasis and resultant symptoms (Fig. 3a). This has recently been discussed for the hip—synovial change is an early sign for hip pain [50]. Comparatively, changes to the open gaps behind the **SIJ** may be predictive of "**SIJ** pain" or more specifically, "*inner SI ligament pain*". This has been demonstrated daily for 30 years with the clinical application of anesthetics to neurovascular bundles in the gaps, to inner ligaments, and also to the **SIJ** (Figs. 2a, 3a) [14, 15, 28, 41, 51].

Involvement of watery fluids in **SI** pain (or "**SIJ** pain") is also suggested by Weber's group [52]. Background noise on MRI is seen as early evidence of **SIJ** disease beneath the joint in elite athletes. Fittingly, we see the **RC/PBSN** nerves very near to the sacral bone (Fig. 3).

Further proof regarding the possible importance of the watery gaps seen here could be the higher substance P content, which for the hip has been measured in patients with pain [53], although there appears to be no such study regarding the **SIJ**.

A main conclusion of our research would be to bring these watery gaps of the **SIJ** region to clinical thinking on what is "**SI** innervation" and thus what "**SI** pain" may be related to. Any hypothetical change of fluids, generally, and in the gaps surrounding the nerves seen here, in our case, may explain, why sacroiliitis (and pain) is related to signs of (painful) ankylosing spondylitis and non-radiographic axial spondyloarthritis, and also to diseases distant from the **SI** region, such as arthritis, enthesitis, and dactylitis and extra-articular diseases such as uveitis, psoriasis, and inflammatory bowel disease—topics on which Winter et al. recently performed an interesting meta-analysis [54].

Conversely, asymptomatic radiological involvement of the **SIJ** is reported to occur in up to 50% of patients with inflammatory bowel disease [55].

Bogduk stated the term "**SI** pain" to be either "ligament pain" or "**SIJ** pain" [28]. Based on our data, we suggest that "**SI** innervation" involves "*inner SI ligament innervation*" and "*outer SI ligament innervation*". In conclusion, while ventral and cranial "**SIJ** innervation" has been discussed [12, 13], dorsal **SIJ** innervation, i.e., innervation of the joint's cartilage, remains unproven.

BIAS and outlook

Possible autonomic involvement by the periarterial plexus of the vessels in the gaps behind the **SIJ** was not investigated, as anticipated by Fortin [13]. Our description of the **RCs/PBSNs** and their branches passing in gaps behind the **SIJ** could be pathological to some extent due to the advanced age of the subjects dissected (median age, 81 years). 61% of German adults have had "back pain" one year ago, of which 15% had chronic pain [56]. Whether the gaps observed are also present in the younger population needs to be reviewed in future studies.

Supplementary Information The online version contains supplementary material available at https://doi.org/10.1007/s00586-022-07353-1.

Acknowledgements We thank Angela Ehrlich for her help in histology. Matthias Oehme, Katja Schmidt and Elisa Schubert helped in organizing the cases. Figure 3a is a scan of PAS serial sections by Dina Wiersbicki's work [23] which we thank for allowance of evaluating the CT and MRI data (Case L51). Case L1 was dissected together with Niels Hammer 2004, further cases with other students. Thomas Wolfskämpf plastinated. Charlotte Kulow proofread the manuscript. The Leipzig and Tokyo body donors were convinced of the importance of anatomy in lifetime: They gave us their bodies. Their trust in our

work is the greatest justification for our gratitude and respect. From their decision, we have freedom of our anatomical research. Thank you.

Funding Open Access funding enabled and organized by Projekt DEAL. The study was partially funded by Deutsche Arthrose-Hilfe e.V. (grant number P425-A687).

Declarations

Conflict of interest The authors declare that they have no competing interests.

Ethics approval This study protocol was approved by the ethics committee of the Medical Faculty at the University of Leipzig, Germany (approval number 398/171-ek) and was conducted in accordance with the 1964 Helsinki Declaration and its later amendments or comparable ethical standards.

Consent to participate While alive, the donors had given consent for the use of their body parts for scientific purposes at the Department of Anatomy of the Tokyo Medical University, and at the Institute of Anatomy, University of Leipzig in accordance with the.

References

1. Clara M (ed) (1953) Das Nervensystem des Menschen. Ein Lehrbuch für Studierende und Ärzte, 2, verbesserte edn. Johann Ambrosius Barth Verlag, Leipzig
2. Ikeda R (1991) Innervation of the sacroiliac joint. Macroscopical and histological studies. Nihon Ika Daigaku Zasshi 58(5):587–596
3. Fortin JD, Washington WJ, Falco FJ (1999) Three pathways between the sacroiliac joint and neural structures. AJNR Am J Neuroradiol 20(8):1429–1434
4. Willard FH, Carreiro JE, Manko W (1998) Third interdisciplinary world congress on low back and pelvic pain. Vienna, Austria: 207–209
5. Szadek KM, Hoogland PV, Zuurmond WW, de Lange JJ, Perez RS (2008) Nociceptive nerve fibers in the sacroiliac joint in humans. Reg Anesth Pain Med 33(1):36–43. https://doi.org/10.1016/j.rapm.2007.07.011
6. Szadek KM, Hoogland PVJM, Zuurmond WWA, de Lange JJ, Perez RSGM (2010) Possible nociceptive structures in the sacroiliac joint cartilage: an immunohistochemical study. Clin Anat 23(2):192–198. https://doi.org/10.1002/ca.20908
7. Vleeming A, Schuenke MD, Masi AT, Carreiro JE, Danneels L, Willard FH (2012) The sacroiliac joint: an overview of its anatomy, function and potential clinical implications. J Anat 221(6):537–567
8. Tubbs RS (ed) (2015) Nerves and Nerve Injuries. Vol. 1: History, Embryology, Anatomy, Imaging, and Diagnostics. Elsevier, Amsterdam, Boston, Heidelberg, London, New York, Oxford, Paris, San Diego, San Francisco, Singapore, Sydney, Tokyo
9. Bogduk N (1983) The innervation of the lumbar spine. Spine 8(3):286–293
10. Saito T, Steinke H, Miyaki T, Nawa S, Umemoto K, Miyakawa K, Wakao N, Asamoto K, Nakano T (2013) Analysis of the posterior ramus of the lumbar spinal nerve: the structure of the posterior ramus of the spinal nerve. Anesthesiology 118(1):88–94. https://doi.org/10.1097/ALN.0b013e318272f40a
11. Saito T, Steinke H (2015) The dorsal rootlets, ventral rootlets, spinal nerve, and rami. In: Tubbs RS (ed) Nerves and Nerve Injuries, vol 1. History, Embryology, Anatomy, Imaging, and Diagnostics. Elsevier, Amsterdam, Boston, Heidelberg, London, New York, Oxford, Paris, San Diego, San Francisco, Singapore, Sydney, Tokyo, pp 451–469
12. Steinke H, Saito T, Miyaki T, Oi Y, Itoh M, Spanel-Borowski K (2009) Anatomy of the human thoracolumbar Rami dorsales nervi spinalis. Ann Anat 191(4):408–416. https://doi.org/10.1016/j.aanat.2009.04.002
13. Fortin JD, Kissling RO, O'Connor BL, Vilensky JA (1999) Sacroiliac joint innervation and pain. Am J Orthop 28(12):687–690
14. Fortin JD, Aprill CN, Ponthieux B, Pier J (1994) Sacroiliac joint. Pain referral maps upon applying a new injection/arthrography technique. Part II: clinical evaluation. Spine 19(13):1483–1489
15. Fortin JD, Dwyer AP, West S, Pier J (1994) Sacroiliac joint. Pain referral maps upon applying a new injection/arthrography technique. Part I: asymptomatic volunteers. Spine 19(13):1475–1482
16. Vilensky JA, O'Connor BL, Fortin JD, Merkel GJ, Jimenez AM, Scofield BA, Kleiner JB (2002) Histologic analysis of neural elements in the human sacroiliac joint. Spine 27(11):1202–1207
17. Fortin JD, Vilensky JA, Merkel GJ (2003) Can the sacroiliac joint cause sciatica? Pain Physician 6(3):269–271
18. Forst SL, Wheeler MT, Fortin JD, Vilensky JA (2006) The sacroiliac joint: anatomy, physiology and clinical significance. Pain Physician 9(1):61–67
19. Vleeming A, Stoeckart R, Volkers AC, Snijders CJ (1990) Relation between form and function in the sacroiliac joint. Part I: Clin Anat Aspects Spine 15(2):130–132
20. Hammer N, Löffler S, Feja C, Sandrock M, Schmidt W, Bechmann I, Steinke H (2012) Ethanol-glycerin fixation with thymol conservation: a potential alternative to formaldehyde and phenol embalming. Anat Sci Educ 5(4):225–233. https://doi.org/10.1002/ase.1270
21. Hammer N, Löffler S, Feja C, Bechmann I, Steinke H (2011) Substitution of formaldehyde in gross anatomy is possible. J Natl Cancer Inst 103(7):610–611. https://doi.org/10.1093/jnci/djr035
22. Hammer N, Löffler S, Bechmann I, Steinke H, Hädrich C, Feja C (2015) Comparison of modified thiel embalming and ethanol-glycerin fixation in an anatomy environment: potentials and limitations of two complementary techniques. Anat Sci Educ 8(1):74–85
23. Wiersbicki D, Völker A, Heyde C-E, Steinke H (2019) Ligamental compartments and their relation to the passing spinal nerves are detectable with MRI inside the lumbar neural foramina. Eur Spine J 28(8):1811–1820. https://doi.org/10.1007/s00586-019-06024-y
24. Steinke H, Wiersbicki D, Speckert M-L, Merkwitz C, Wolfskämpf T, Wolf B (2018) Periodic acid-Schiff (PAS) reaction and plastination in whole body slices. A novel technique to identify fascial tissue structures. Ann of Anat—Anatomischer Anzeiger 216:29–35. https://doi.org/10.1016/j.aanat.2017.10.001
25. Kürtül I, Hammer N, Rabi S, Saito T, Böhme J, Steinke H (2012) Oblique sectional planes of block plastinates eased by Sac Plastination. Ann Anat 194(4):404–406. https://doi.org/10.1016/j.aanat.2011.11.006

26. Hammer N, Steinke H, Slowik V, Josten C, Stadler J, Böhme J, Spanel-Borowski K (2009) The sacrotuberous and the sacrospinous ligament–a virtual reconstruction. Ann Anat—Anatomischer Anzeiger 191(4):417–425. https://doi.org/10.1016/j.aanat.2009.03.001
27. Steinke H, Hammer N, Slowik V, Stadler J, Josten C, Bohme J, Spanel-Borowski K (2010) Novel insights into the sacroiliac joint ligaments. Spine 35(3):257–263. https://doi.org/10.1097/BRS.0b013e3181b7c675 (**Phila Pa 1976**)
28. Bogduk N (2017) A commentary on appropriate use criteria for sacroiliac pain. Pain Med 18(11):2055–2057
29. Pernkopf E (1943) Bauch, Becken und Beckengliedmaße. Urban und Schwarzenberg, Berlin, Wien
30. Saito T, Yoshimoto M, Yamamoto Y, Miyaki T, Itoh M, Shimizu S, Oi Y, Schmidt W, Steinke H (2006) The medial branch of the lateral branch of the posterior ramus of the spinal nerve. Surg Radiol Anat 28(3):228–234. https://doi.org/10.1007/s00276-006-0090-3
31. Hungerford B, Gilleard W, Hodges P (2003) Evidence of altered lumbopelvic muscle recruitment in the presence of sacroiliac joint pain. Spine 28(14):1593–1600
32. McGrath C, Nicholson H, Hurst P (2009) The long posterior sacroiliac ligament. A histological study of morphological relations in the posterior sacroiliac region. Joint Bone Spine 76(1):57–62. https://doi.org/10.1016/j.jbspin.2008.02.015
33. Anheyer D, Haller H, Lauche R, Dobos G, Cramer H (2021) Yoga for treating low back pain. A systematic review and meta-analysis. Pain. https://doi.org/10.1097/j.pain.0000000000002416
34. Hammer N, Steinke H, Bohme J, Stadler J, Josten C, Spanel-Borowski K (2010) Description of the iliolumbar ligament for computer-assisted reconstruction. Ann Anat 192(3):162–167. https://doi.org/10.1016/j.aanat.2010.02.003
35. Bechtel R (2001) Physical characteristics of the axial interosseous ligament of the human sacroiliac joint. Spine J 1(4):255–259
36. Cox M, Ng G, Mashriqi F, Iwanaga J, Alonso F, Tubbs K, Loukas M, Oskouian RJ, Tubbs RS (2017) Innervation of the anterior sacroiliac joint. World Neurosurg 107:750–752. https://doi.org/10.1016/j.wneu.2017.08.062
37. Kibsgård TJ, Röhrl SM, Røise O, Sturesson B, Stuge B (2017) Movement of the sacroiliac joint during the Active Straight Leg Raise test in patients with long-lasting severe sacroiliac joint pain. Clin Biomech (Bristol, Avon) 47:40–45. https://doi.org/10.1016/j.clinbiomech.2017.05.014
38. Hammer N, Scholze M, Kibsgård T, Klima S, Schleifenbaum S, Seidel T, Werner M, Grunert R (2019) Physiological in vitro sacroiliac joint motion. A study on three-dimensional posterior pelvic ring kinematics. J Anat 234(3):346–358. https://doi.org/10.1111/joa.12924
39. Konno T, Aota Y, Saito T, Qu N, Hayashi S, Kawata S, Itoh M (2017) Anatomical study of middle cluneal nerve entrapment. J Pain Res 10:1431–1435. https://doi.org/10.2147/JPR.S135382
40. Foley BS, Buschbacher RM (2006) Sacroiliac joint pain. Anatomy, biomechanics, diagnosis, and treatment. Am J Phys Med Rehabil 85(12):997–1006. https://doi.org/10.1097/01.phm.0000247633.68694.c1
41. Vandervennet W, van Boxem K, Peene L, Mesotten D, Buyse K, Devooght P, Mestrum R, Puylaert M, Vanlantschoot A, Vanneste T, van Zundert J (2021) Does the presence of cranial contrast spread during a sacroiliac joint injection predict short-term outcome? Reg Anesth Pain Med 46(3):217–221. https://doi.org/10.1136/rapm-2020-101673
42. Applegate WV, Buckwalter NR (1997) Microanatomy of the structures contributing to abdominal cutaneous nerve entrapment syndrome. J Am Board Fam Pract 10(5):329–332
43. Messina A, Messina JC (1995) Transposition of the ulnar nerve and its vascular bundle for the entrapment syndrome at the elbow. J Hand Surg 20(5):638–648. https://doi.org/10.1016/S0266-7681(05)80126-3
44. Steinke H, Rabi S, Saito T (2008) Staining body slices before and after plastination. Europ J Anat 12(1):51–55
45. Gartenberg A, Nessim A, Cho W (2021) Sacroiliac joint dysfunction Pathophysiology, diagnosis, and treatment. Eur Spine J 30(10):2936–2943. https://doi.org/10.1007/s00586-021-06927-9
46. Fukada E, Ueda H, Rinaldi R (1976) Piezoelectric and related properties of hydrated collagen. Biophys J 16(8):911–918. https://doi.org/10.1016/S0006-3495(76)85741-4
47. Fullerton GD, Amurao MR (2006) Evidence that collagen and tendon have monolayer water coverage in the native state. Cell Biol Int 30(1):56–65
48. Gerli MFM, Guyette JP, Evangelista-Leite D, Ghoshhajra BB, Ott HC (2018) Perfusion decellularization of a human limb: a novel platform for composite tissue engineering and reconstructive surgery. PLoS ONE 13(1):e0191497
49. Ott HC, Clippinger B, Conrad C, Schuetz C, Pomerantseva I, Ikonomou L, Kotton D, Vacanti JP (2010) Regeneration and orthotopic transplantation of a bioartificial lung. Nat Med 16(8):927–933
50. Mayes S, Ferris A-R, Smith P, Cook J (2020) Hip joint effusion-synovitis is associated with hip pain and sports/recreation function in female professional ballet dancers. Clin J Sport Med : Official J Canadian Acad Sport Med 30(4):341–347. https://doi.org/10.1097/JSM.0000000000000595
51. Vleeming A, Albert HB, Ostgaard HC, Sturesson B, Stuge B (2008) European guidelines for the diagnosis and treatment of pelvic girdle pain. Eur Spine J 17(6):794–819. https://doi.org/10.1007/s00586-008-0602-4
52. Weber U, Jurik AG, Zejden A, Larsen E, Jørgensen SH, Rufibach K, Schioldan C, Schmidt-Olsen S (2018) Frequency and anatomic distribution of magnetic resonance imaging features in the sacroiliac joints of young athletes. Exploring "Background Noise" toward a data-driven definition of sacroiliitis in early spondyloarthritis. Arthritis Rheumatol 70(5):736–745. https://doi.org/10.1002/art.40429
53. Wang H, Zheng X-F, Zhang X, Li Z, Shen C, Zhu J-F, Cui Y-M, Chen X-D (2014) Increasing substance P levels in serum and synovial tissues from patients with developmental dysplasia of the hip (DDH). BMC Musculoskelet Disord 15(1):1–8
54. de Winter JJ, van Mens LJ, van der Heijde D, Landewé R, Baeten DL (2016) Prevalence of peripheral and extra-articular disease in ankylosing spondylitis versus non-radiographic axial spondyloarthritis. A Meta-Analysis Arthritis Res Therapy 18:196. https://doi.org/10.1186/s13075-016-1093-z
55. Salvarani C, Fries W (2009) Clinical features and epidemiology of spondyloarthritides associated with inflammatory bowel disease. World J Gastroenterol 15(20):2449–2455. https://doi.org/10.3748/wjg.15.2449
56. von der Lippe E, Krause L, Prost M, Wengler A, Leddin J, Müller A, Zeisler M-L, Anton A, Rommel A (2021) Prävalenz von rücken-und nackenschmerzen in deutschland. J Health Monit. https://doi.org/10.25646/7854